Interfacial Crack Propagation Under Various Mode-Mixes

Byung-Sun Choi, Young-Suck Chai*
School of Mechanical Engineering, Yeungnam University, Gyongsan, Kyungbook 712-749, Korea

Initiation and propagation of interfacial crack along bimaterial interface are considered in this study. A biaxial loading device for a single specimen is used for obtaining a wide range of mode-mixities. The specimen is an edge-cracked bimaterial strip of glass and epoxy; the biaxial loading device, being capable of controlling displacements in two perpendicular directions, is developed. A series of interfacial crack initiation and propagation experiments are conducted using the biaxial loading device for various mixed modes. Normal crack opening displacement (NCOD) is measured near crack front by a crack opening interferometry and used for extracting fracture parameters. From mixed mode interfacial crack initiation experiments, large increase in toughness with shear components is observed. The behavior of interfacial crack propagation analyzed as a function of mode-mix shows that initial crack propagation is delayed with increase of mode-mixity, and its velocity is increased with positive mode-mixity but decreased with negative case. However, it is found that crack propagation is less accelerated with positive mode-mixity than the negative mode-mixity, which may be caused by contact and/or effects of friction between far field and near-tip field along the interfacial crack.

Key Words : Interfacial Crack, Bimaterial, Mode-Mixity, Fracture Parameter, Crack Opening Interferometry

1. Introduction

Structural reliability of composite materials can be strongly affected by the fracture toughness of interface between two constituents. The failure of interface is inherently a mixed mode problem, particularly when crack is constrained to grow along the interface because of the mismatch of material properties across the interface. If composite materials or devices compromising two or more materials are to be designed to resist interfacial cracking, then criteria governing initiation and growth under mixed modes must be established. Since a work of Malyshev and Salganik (1965), a number of studies (Liechti, 1988; Cao, 1989; Wang, 1990) of mixed mode effects on interfacial toughness have been conducted. Recently, Liechti and Chai (1991, 1992) developed a bimaterial interfacial fracture specimen of epoxy and glass that can generate interface toughness function. They observed that the overall interfacial toughness increased with the shear component of fracture mode. They considered the energy dissipation and surface asperities to show the reason of increase in toughness but failed to explain clearly.

The objective of this research is to examine mixed mode interfacial crack propagation along bimaterial interface. Approach for obtaining a wide range of mode-mixes is to use a single specimen of glass-epoxy in conjunction with a biaxial loading device. The crack opening interferometry technique is used to measure the normal crack opening displacement (NCOD) of which profiles are recorded. The results of interfacial crack propagation experiments over a

* Corresponding Author,
E-mail : yschai@yu.ac.kr
TEL : +82-53-810-2464; **FAX** : +82-53-813-3703
School of Mechanical Engineering, Yeungnam University, Gyongsan, Kyungbook 712-749, Korea. (Manuscript **Received** March 12, 2001; **Revised** October 25, 2001)

wide range of mode-mixes are presented in this study.

2. Experiments

2.1 Parameters

Just ahead of the interfacial crack-tip at a distance r along $\theta=0$, stresses are given by (Rice, 1988)

$$\sigma_{22}+i\sigma_{12}=\frac{Kr^{i\varepsilon}}{\sqrt{2\pi r}} \quad (1)$$

where K is a complex stress intensity factor defined as $K=K_1+iK_2$ and the bimaterial constant, ε is (Rice, 1988)

$$\varepsilon=\frac{1}{2\pi}\ln\left[\frac{\chi_1\mu_2+\mu_1}{\chi_2\mu_1+\mu_2}\right] \quad (2)$$

where μ is the shear modulus and χ is defined as $(3-4\nu)$ for plane strain and $(3-\nu)/(1+\nu)$ for plane stress. The subscripts 1 and 2 refer to the upper and lower materials, respectively. The mode-mix, Ψ is defined as

$$\Psi=\tan^{-1}\left[\frac{K_2}{K_1}\right] \quad (3)$$

Energy release rate for plane strain can be obtained from complex stress intensity factor through (Rice, 1988)

$$G=\frac{1}{4\cosh^2\pi\varepsilon}\left[\frac{1-\nu_1}{\mu_1}+\frac{1-\nu_2}{\mu_2}\right](K_1^2+K_2^2) \quad (4)$$

2.2 Specimen and experimental device

The purpose of this work is to clarify the behavior of interfacial crack propagation in terms of mode-mix. A combined experimental and numerical method was used to elucidate interfacial debonding mechanism. A single specimen geometry in conjunction with a biaxial loading device was used for obtaining a wide range of fracture mode-mixes. The specimen geometry selected was an edge-cracked bimaterial strip, showing a wide range of mode-mixes. It is well known for its linear compliance vs. crack length relation for a sufficiently long crack and the crack length independence of fracture parameters. The specimen geometry and loading are shown in Fig. 1, which is made up of epoxy and glass. Material properties used in analysis are listed in Table 1.

Table 1 Material Properities

Material	Young's Modulus E(GPa)	Poisson's ratio ν
Epoxy	1.97	0.33
Glass	68.95	0.20

Dundur's Parameters : $\alpha=-0.9402772$, $\beta=-0.2349565$

Bimaterial constant : $\varepsilon=0.07621267$

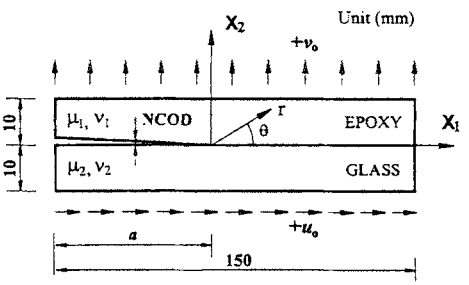

Fig. 1 Bimaterial edge-cracked strip specimen

A development of biaxial delamination tester, which is capable of controlling displacements in two perpendicular directions to the specimen, and the measurement of normal crack opening displacements (NCOD) by crack opening interferometry are described. Due to the low toughness of epoxy-glass interface, applied displacements should be controlled with high resolution. Furthermore, it was important to minimize interaction between two loading directions. The stiffness of loading device was high enough so that crack initiation process (slow extension) and growth could be examined. Finally, normal crack opening displacement (NCOD) was measured to examine inelastic, three-dimensional and/or contact effects in the crack tip region where microscope access was provided.

A schematic of the biaxial delamination tester is shown in Fig. 2. The specimen was glued along the edges to two sets of grip plates which were connected to a linear bearing and actuators. Two types of loading conditions - normal loading of bond normal displacements and sequential loading of positive or negative bond tangential displacements followed by bond normal displacements until debonding - are applied in this study as shown in Fig. 3.

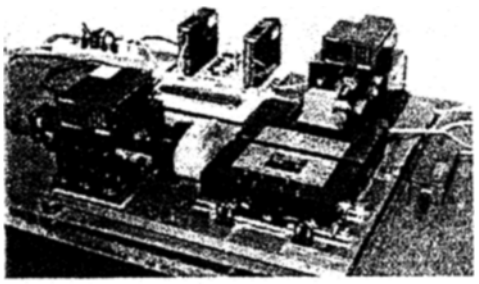

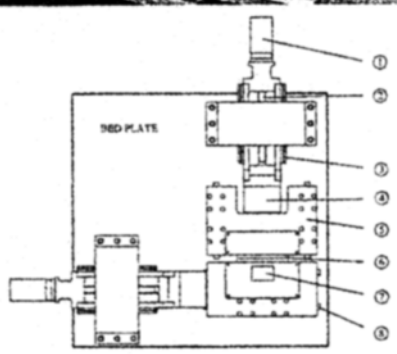

Fig. 2 Biaxial delamination tester

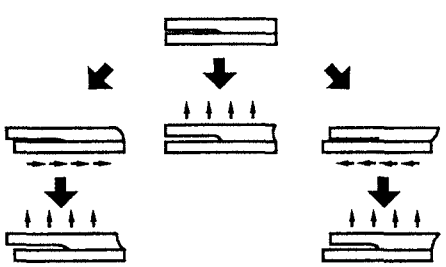

Fig. 3 Applied loading condition at specimen

In addition to the measurements of load and displacement, NCOD was measured near crack front using crack opening interferometry. A schematic of crack opening interferometry employed in this study was shown in Fig. 4. A 45° mirror was mounted on one of the grips to introduce a laser light through glass for reflection by the crack faces. The reflected beams interfered to form the resulting fringe patterns which were caught and resolved by a microscope as Fig. 5. For the normal incidence, a dark fringe of order m is a contour of NCOD, Δv, given by

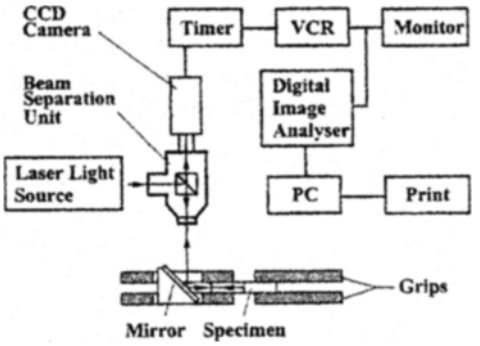

Fig. 4 Crack opening interferometry

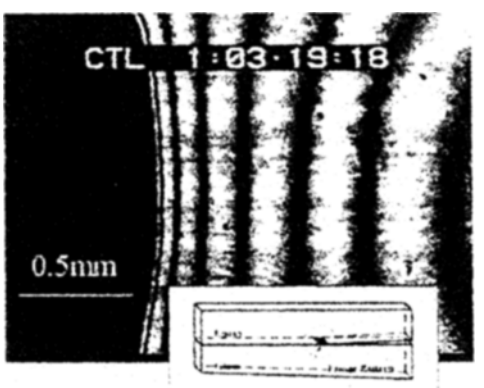

Fig. 5 Typical fringe pattern

$$\Delta v = m\frac{\lambda}{2} \tag{5}$$

The wavelength λ of He-Ne laser, was 632.8 *nm*, yielding a resolution per half fringe (bright to dark) of 158.2 *nm*. The fringe patterns were recorded through a video camera and timer onto a high resolution video cassette recorder. The records were later analyzed using a digital image analyzer system to obtain light intensity profiles along the center of the specimen. The intensity profiles were then filtered prior to thresholding in order to determine fringe locations. The whole procedure and fringe counting scheme were automated so that NCOD profiles could be obtained. The video timer allowed the NCOD measurements to be synchronized with those of the applied displacements and reactions.

3. Toughness of Interfacial Crack

A series of experiments applying normal

loadings and sequential loadings were conducted. A sequence of NCOD profiles was taken from the center of a series of interference patterns, corresponding to the center of a specimen, far from any edge effect. The NCOD data, alone, do not provide sufficient information to extract mixed mode fracture parameters, particularly during crack initiation. A hybrid experimental/finite element analysis procedure was implemented. The procedure consists of matching the measured NCOD and finite element solutions in a near tip region and then using the matched finite element solutions to extract mixed mode fracture parameters. In order to extract complex stress intensity factor, several techniques such as crack opening displacement (Smelser, 1979), virtual crack closure (Raju, 1986) and conservation integral technique (Yau, 1984) were compared, and the last was found to be most satisfactory, which was incorporated as a post-processing routine in the finite element code ABAQUS. The auxiliary solutions required for the technique were taken from the result by Smelser (1979). Once the complex stress intensity factors were found, Eqs. (3) and (4) were used to determine mixed mode interfacial fracture parameters, such as mode mixity, Ψ, critical energy release rate, G_c, during crack initiation.

The interfacial fracture toughness was plotted as a function of mode-mixity, Ψ, in Fig. 6. The results were obtained from six specimens with some overlap in mode-mix from specimen to specimen. Interfacial fracture toughness was extracted from the above mentioned routine with ABAQUS output, and collected from each experiment. The experiments that were analyzed were part of a series of experiments that was conducted over a range of mode-mixes from $-45° < \Psi < 60°$. The range was provided by applying various levels of tangential displacements followed by normal displacements until crack propagation occurred. It was observed that there was a large increase in interfacial toughness with shear components as noted by a number of investigators (Liechti, 1988; Cao, 1989; Wang, 1990; Liechti, 1991; Liechti, 1992). Another interesting feature is that the degree of shielding provided by positive and negative in-plane shear is asymmetric.

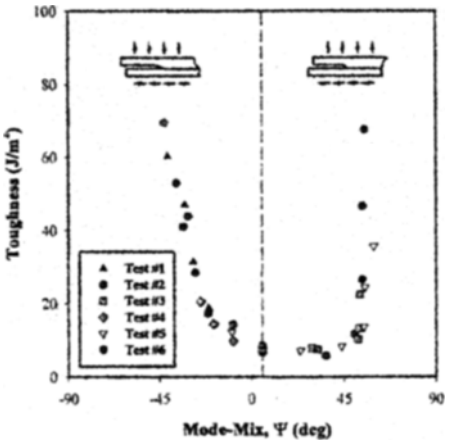

Fig. 6 Variation of interfacial toughness with mode-mix

4. Results

4.1 Interfacial crack propagation

The several processes of crack propagation are shown in Fig. 7 and Fig. 8. Either positive or negative mode-mixity is noted in upper-case or lower-case letters, respectively. Neglecting time for applied shear displacement, the processes were plotted from when the normal displacement was applied. Mode-mixities just before crack initiation were also presented.

With regard to positive mode-mixes, several processes of crack propagation are shown in Fig. 7. The rate of displacement applied to specimen is 0.5μm/sec. In the case of "A", pure normal displacement is applied. As normal displacements are increased, initial crack starts to delaminate after about 23 seconds. The crack grows more rapidly with further application of normal displacements. From the cases "A" to "G", the amounts of shear displacements, i. e. mode-mixes, are increased. It could be shown that as mode-mix grows larger, crack propagation pattern shows some different aspects. According to the results, it could be noted as the amount of positive mode-mix increases, crack propagation makes a more rapid progress while crack initiation shows

slower starting. In comparison with cases "A" to "E", the case "F" of having more shear components shows more delayed crack initiation and crack propagation starts rather abruptly. In this case, crack propagation seems to be restrained before it bursts out after accumulating adequate energy. In the case of "G", this is more apparent and its abrupt crack progression was surprisingly rapid.

The results seen in Fig. 8 show several types of crack propagation in terms of negative mode-mixes. In order to compare with the case of positive mode-mix in Fig. 7, the results are shown graphically in conjunction with the case to which pure normal displacement is applied. The results from "a" to "g" allow us to find that the initial crack starts more slowly as the increase negative mode-mix. The crack propagation pattern in case of negative mode-mix consists of two parts of primary and secondary stages. The feature is more apparent with the help of Fig. 11 which describes interfacial crack velocity. The results show that as the increase of negative mode-mix, the velocity of crack propagation at primary stage is slower. Nevertheless, the crack propagation at the latter part of secondary stage is seen to be quite rapid. In the particular case of "d", crack propagation goes up sharply around after 67 seconds while the initial crack propagation starts slowly as shown in cases "a" through "c". In the case of "e", crack initiation begins a bit late and makes a very slow progress at primary stage as similar to the case "d". At the latter part of secondary stage, the crack propagation, however, is made abruptly just like in the case of "d". These trends of crack propagation also seems to be prevented before the unstable crack growth. In the cases of "f" and "g" which have relatively more shear components, these prohibitive properties come to be cleared and the crack propagation continues to be made without interruption. Particularly, the crack propagation in these cases was too fast to be controlled by the testing equipment.

The zero point in Fig. 9 was shifted from the point where crack propagation is initiated in Fig. 7 and 8. The results in Fig. 9 show that the initial crack propagation is made more rapidly as an increase of positive mode-mix and vice versa with the increase of negative mode-mix. Accordingly, it can be inferred from the results that the initial crack propagation at large depends upon the mode-mixes.

According to the results mentioned above, as the increase of both positive and negative mode-mixes, crack propagation seems to be prohibited before it bursts out to steady propagation. In several cases of large components of positive mode-mixes, the stick-slip behavior of which the crack develops, stops and then resumes with propagation (marking ◯) as in Fig. 10 could be reported. This attests to the fact that the crack propagation was prohibited and then found its way around into ensuing development. In observing a variety of aspects of crack propagation, it can be concluded that the interfacial crack propagation was interfered by contact, frictional locking mechanisms. And also,

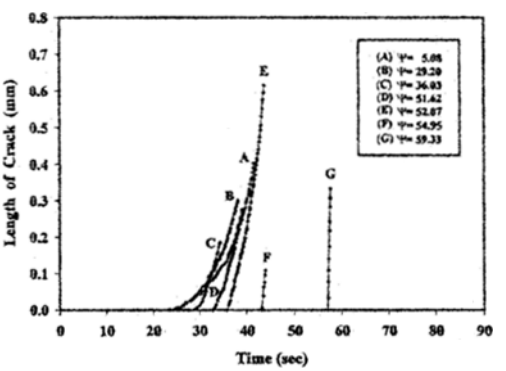

Fig. 7 Behavior of interfacial crack propagation under positive mode-mix

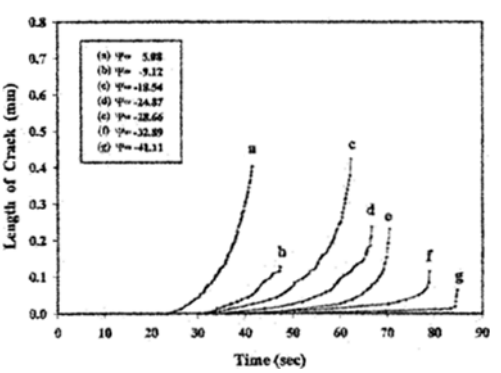

Fig. 8 Behavior of interfacial crack propagation under negative mode-mix

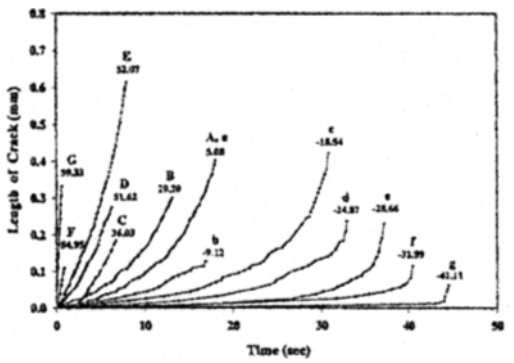

Fig. 9 Behavior of interfacial crack propagation with mode-mix

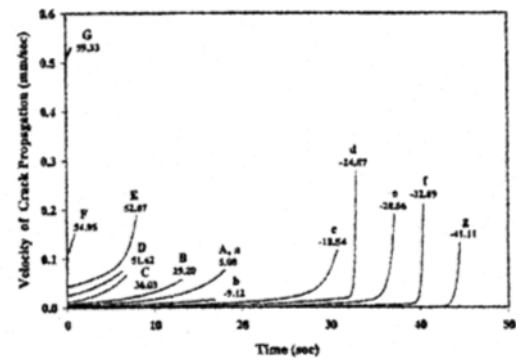

Fig. 11 Velocity of interfacial crack propagation with mode-mix

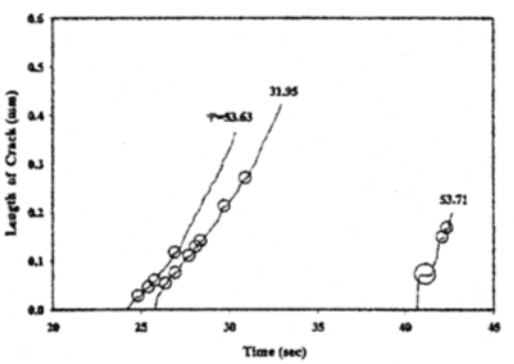

Fig. 10 Stick-slip behavior in interfacial crack propagation

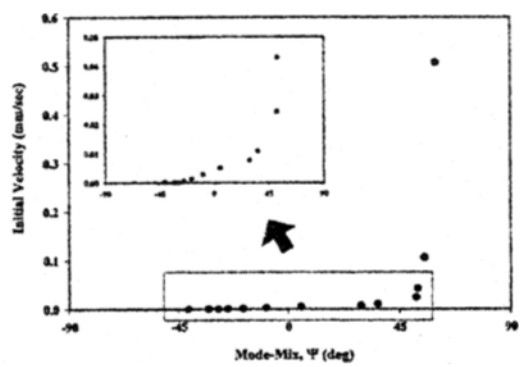

Fig. 12 Initial velocity of crack propagation with mode-mix

the enlargement of contact area with the increase of mode-mix also contributed mainly to the interference of crack propagation.

4.2 Crack propagation velocity

To find out the variation of velocity in interfacial crack propagation, the results in Fig. 9 are curve-fitted. The standard deviation error in data during curve-fitting procedure was 0.0025 ~0.0069, considerably smaller than expected.

Figure 11 shows the velocity diagram of interfacial crack propagation with respect to the mode-mix which results from differentiating the curve-fitted results in Fig. 9. In Fig. 11, the behavior of interfacial crack propagation can be clearly seen. The Initial velocity of crack propagation with variation of different mode-mix is described more detail in Fig. 12. It can be concluded that, the velocity of initial crack propagation is more rapid as increase of positive mode-mix. The initial velocity of crack propagation with the increase of negative mode-mix, however, is shown as opposite results. In the case of positive mode-mixes in "F" and "G", their initial crack propagations are very rapid, but their increase rates are not very large. On the other hand, in the case of negative mode-mixes in "d" through "g", increase rates are so high. In the steady process of crack propagation, it could be seen that there were relatively gradual acceleration with large component of positive mode-mix and the sudden acceleration with large component of negative mode-mix.

5. Conclusions

A series of interfacial crack initiation and propagation experiments using the glass-epoxy

edge-cracked bimaterial strip were analyzed as a function of mode-mix and the following conclusions are made.

- From the interfacial crack initiation experiments, it could be seen that there was a large increase in toughness with shear components and the degree of shielding provided by positive and negative in-plane shear is asymmetric.
- Interfacial crack propagation results show that the initial crack propagation was delayed as increase of absolute value of positive or negative mode-mix while the steady propagation makes a more rapid progress with the increase of mode-mix.
- Initial velocity of crack propagation is very dependent upon the mode-mixes. It increased with positive mode-mix and decreased with negative mode-mix. Crack propagation was less accelerated with positive mode-mix than the negative mode-mix.
- In several cases of large components of positive mode-mixes, the stick-slip behavior during interfacial crack propagation was inspected.
- Possible reasons of the increase in toughness with mode-mix might be effects of friction, locking mechanism and contact area due to contact behavior along the interfacial crack.

Acknowledgements

This work was supported by the Brain Korea 21 Projects in 2000 and 2001

References

ABAQUS User's Manual Version 4. 7, 1999, Hibbit, Karlsson and Sorensen, Inc.

Cao, H. C. and Evans, A. G., 1989, "An Experimental Study of the Fracture Resistance of Bimaterial Interfaces," *Mechanics of Materials*, Vol. 7, pp. 295~304.

Liechti, K. M. and Hanson, E. C., 1988, "Nonlinear Effects in Mixed-mode Interfacial Delaminations," *Int. J. Fract.*, Vol. 36, pp. 199~217.

Liechti, K. M. and Chai, Y. S., 1991, "Biaxial Loading Experiments for Determining Interfacial Fracture Toughness," *J. Appl. Mech.*, Vol. 58, pp. 680~687.

Liechti, K. M. and Chai, Y. S., 1992, "Asymmetric Shielding in Interfacial Fracture Under In-Plane Shear," *J. Appl. Mech.*, Vol. 59, pp. 295~304.

Malyshev, B. M. and Salganik, R. L., 1965, "The Strength of Adhesive Joints Using the Theory of Cracks," *Int. J. Fract. Mech.*, Vol. 1, pp. 114~128.

Raju, I. S., 1986, "Simple Formulas for Strain Energy Release Rates with Higher Order and Singular Finite Elements," *NASA Contractor Report 178186.*

Rice, J. R., 1988, "Elastic Fracture Mechanics Concepts for Interfacial Cracks," *J. Appl. Mech.*, Vol. 55, pp. 98~103.

Smelser, R. E., 1979, "Evaluation of Stress Intensity Factors for Bimaterial Bodies Using Numerical Crack Flank Displacement Data," *Int. J. Fract.*, Vol. 15, pp. 135~143.

Wang, J. S. and Suo, Z., 1990, "Experimental Determination of Interfacial Toughness Using Brazil-Nut-Sandwich," *Acta. Metal.*, Vol. 38, pp. 1279~1290.

Yau, J. F. and Wang, S. S., 1984, "An Analysis of Interface Cracks between Dissimilar Isotropic Materials Using Conservation Integrals in Elasticity," *Eng. Fract. Mech.*, Vol. 20, pp. 423~432.